Effect of Chirality on the Structural Behaviour of Hydrogen-Bonded *n*-Alkylammonium Pyroglutamates in the Crystalline and Smectic State

Dimitris Tsiourvas,*[a] Constantinos M. Paleos,[a] and Antoine Skoulios*[b]

Abstract: A set of optically active and racemic *n*-alkylammonium pyroglutamates from dodecyl to octadecyl were synthesized and characterised. Their thermotropic polymorphism was investigated by polarizing optical microscopy, differential scanning calorimetry and dilatometry. Their structure in the crystalline and smectic state was analysed by X-ray diffraction. The hydrogen bonding of the molecules in the crystalline and smectic layers was examined by infrared spectroscopy. The chirality control over the supramolecular self-assembly of the molecules along with the homochiral and heterochiral architecture of the self-assembled dimers are briefly discussed.

Keywords: amino acids · chirality · liquid crystals · self-assembly · supramolecular chemistry

Introduction

A straightforward and facile method of producing mesogenic compounds is to attach ionic headgroups onto paraffin chains, by neutralising, for instance, long-chain alkylamines with halides of divalent metals,[1, 2] halogen acids,[3–5] or high-molecular-weight polyacids.[6–8] Another method is to use hydrogen bonding to either command directly the positional register of the molecules within layers or columns, or else simply to reinforce this register in a two-level process by combining hydrogen bonding with ionic interactions.[9–11] The latter method was successfully used in recent work on the preparation of smectic liquid crystals from *n*-alkylammonium salts of L-pyroglutamic acid (abbreviated in the following to L*n*, in which *n* is the number of carbon atoms in the alkyl chains).[12] In these liquid crystals, the layering of the ionic molecules is clearly favoured by the hydrogen bonding of the pyroglutamic groups, which doubles the length of the rigid polar parts of the molecules and so enhances the amphiphilic character.

Chiral liquid crystals have been extensively investigated both experimentally and theoretically, because of their special properties and also their potential technological applications.[13] Optical purity has been found to have an incisive effect upon the liquid crystalline behaviour,[14–16] which sometimes leads to the formation of additional liquid crystal phases at intermediate optical purities.[17–18] To study this question in the case of the alkylammonium pyroglutamates, we decided to complete our previous study of the optically active L*n* compounds[12] with a study of their "racemic" counterparts (abbreviated in the following to DL*n* and synthesized in the same way as the L*n* compounds; see Experimental Section). We also studied their binary mixtures at various compositions.

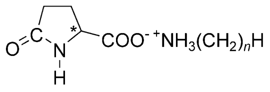

n = 12, 14, 16, 18

Results and Discussion

Preliminary remarks: Before reporting and analysing the experimental data collected in the present work, it is useful to emphasise two important molecular characteristics of the pyroglutamic groups. Firstly, because of the presence of an asymmetric carbon atom in the molecule, pyroglutamic acid can exist in two stereochemically distinct enantiomeric forms: the levorotatory L form, $[\alpha]_D^{20} = -11.9$ ($c = 2$ in H_2O),[19] in which the carboxylic group attached to the asymmetric carbon atom points above the pyrrolidone ring, and the dextrorotatory D form, in which it points below.

---

[a] Dr. D. Tsiourvas, Dr. C. M. Paleos
Institute of Physical Chemistry, NCSR "Demokritos"
15310 Aghia Paraskevi, Attiki (Greece)
Fax: (+30)2106529792
E-mail: tsiourvas@chem.demokritos.gr

[b] Dr. A. Skoulios
Groupe des Matériaux Organiques
Institut de Physique et Chimie des Matériaux
23, rue du Loess, 67037 Strasbourg (France)
E-mail: skoulios@ipcms.u-strasbg.fr

Supporting information for this article is available on the WWW under http://www.chemeurj.org or from the author.

DOI: 10.1002/chem.200304985

It is well known that the D and L enantiomers of any chiral compound have the same crystal structure in the solid state;[20] the D and L structures are merely mirror images of one another. Their equimolar mixture can present itself either as a mechanical mixture of D and L crystals (conglomerate), as a solid solution (pseudoracemate), or finally as a distinct crystalline system (true racemic) with the D and L molecules associated in pairs and related to each other through at least one inverse element of symmetry (centre, mirror, inverse axis).

On the other hand, because of the presence of an amide group in the molecules, the pyroglutamate groups are susceptible to dimerization through dihapto hydrogen bonding. As established by FTIR spectroscopy from the presence of N–H stretching vibrations at about 3200 cm^{-1},[21] the L*n* and DL*n* compounds are, for all practical purposes, completely dimerized in the temperature range explored in the present work.

Molecular modelling (Hyperchem software) indicates that the L*n* and DL*n* dimers have roughly the shape of "bricks" about 11 Å long, 7 Å wide and 4.4 Å thick (Figure 1). The carboxylate groups in the LL dimers stick outwards from the corners of the bricks and both point to the same side with respect to the average pyrrolidone plane, while they point to opposite sides in the DL dimers. In the optically active L*n* compounds, which are made entirely of L enantiomers, the dimers are of course all of the LL type. However, in the "racemic" DL*n* salts, the dimers may equally well be DL, LL or DD in nature. In the present study we will investigate whether the crystal and smectic phases consist of entirely DL, or of DD and LL dimers associated in pairs.

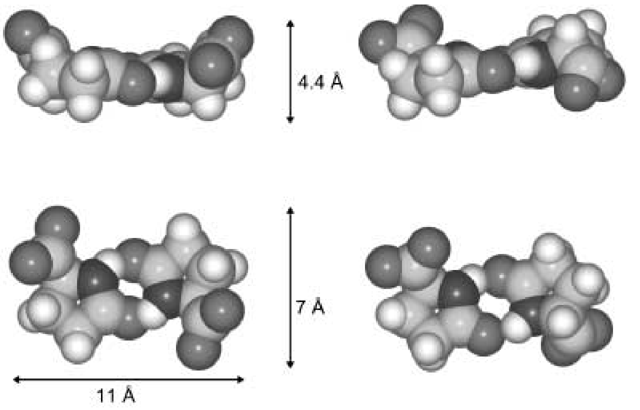

Figure 1. Side view (top) and top view (bottom) of a dimerized LL (left) and DL (right) pyroglutamate group generated with Hyperchem molecular modelling.

Thermal stability: The DL*n* and L*n* compounds were all found to be thermally stable by thermogravimetry over a relatively wide range of temperatures, and only started to degrade slowly at temperatures higher than about 140 °C. Special care must therefore be taken in their study, especially in the time-consuming differential scanning calorimetry (DSC) and dilatometry experiments, to avoid inconsiderately prolonged heating at high temperatures. Sometimes, the heating of optically active compounds at high temperature induces racemization. However, this is definitely not the case of the L*n* compounds, and was checked by measuring the specific rotation of L18 before and after a 10-min heating in the bulk at 130 °C: $[\alpha]_D^{25} = -3.5$ ($c = 2$ in ethanol).

The thermal stability of the hydrogen-bonded L*n* and DL*n* dimers was finally checked by FTIR spectroscopy, with reference to dimers from cyclic lactams with a *cis* configuration. In the low-temperature crystalline state, the hydrogen bonding is revealed by the presence in the spectra of two rather sharp bands at 3228 and 1679 cm^{-1} for L*n*, and 3235 and 1682 cm^{-1} for DL*n*. The first band originates from the N–H stretching vibrations of the secondary amide groups and the second one from the amide I vibrations (C=O stretching coupled mainly with the C–N stretching mode). In the high-temperature smectic phase,[12] both bands broaden out and shift to higher frequencies: 3245 and 1685 cm^{-1} respectively. The shifts observed are, however, very small. For instance, the N–H band remains a long way from that observed at 3433 cm^{-1} in very dilute solutions of L*n* and DL*n* in apolar solvents, in which the dimers are strongly, though not completely, dissociated. Quite clearly, hydrogen bonding continues to prevail in the smectic state; the band broadening observed is probably due to enhanced molecular motions in the fluid mesophase and not to a major weakening of the strength of the oscillators.

Optical textures: The liquid crystal character of the L*n* and DL*n* compounds was investigated by polarizing optical microscopy. Upon heating, the materials exhibit two distinct phase transitions at well-defined temperatures depending upon chirality and alkyl chain length: one from the crystal into a liquid crystal and another one from the liquid crystal into an isotropic melt. Upon cooling from the isotropic melt, well-developed, fan-shaped, focal-conic textures are observed, which indicate the smectic nature of the liquid crystal phases. When inserted between glass plates treated with octadecyltrichlorosilane to achieve homeotropic alignment of the molecules, these smectic phases give no sign of birefringence, revealing their uniaxial smectic A character.

Thermal behaviour: The DSC measurements performed are summarised in Table 1. They carry over to the following comments and remarks. The smectic-to-isotropic phase tran-

Table 1. Transition temperatures (onset) [°C] and enthalpies [kJ mol^{-1}] of the DL*n* and L*n* compounds measured by DSC on heating.[a]

	T_s		ΔH_s		T_i		ΔH_i	
n	DL*n*	L*n*	DL*n*	L*n*	DL*n*	L*n*	DL*n*	L*n*
12	111.5	72.5	40.5	41.5	113.0	113.0	0.8	0.8
14	112.0	81.0	46.0	50.0	144.5	145.5	1.0	1.0
16	113.5	86.5	51.0	59.0	158.5	158.0	1.1	1.1
18	114.5	91.0	57.0	68.5	162.0	162.0	1.0	1.2

[a] Subscripts s and i refer to the crystal–smectic and smectic–isotropic phase transitions, respectively. Data for L*n* are taken from ref. [12]. Owing to thermal degradation, the T_i temperatures measured by DSC are less precise and globally smaller by some 3–5 °C than those measured by optical microscopy.

sition temperatures and enthalpies of the DL*n* compounds are, within experimental error, identical to those of the optically active L*n* analogues. This implies that the amphiphilic character of the molecules, that is, the tendency of the pyroglutamate groups to segregate from the alkyl chains in the smectic state, is not affected by chirality in a perceptible way. On the other hand, these temperatures grow strongly with the length of the alkyl chains, indicating that the effective repulsions between the pyroglutamic cores and the alkyl chains never stop developing in the range of the chain lengths explored.

The crystal-to-smectic phase transition temperatures of the DL*n* compounds are significantly higher (by as much as 20–40 °C) than those of the corresponding L*n* analogues (Table 1). This suggests that in the solid state the DL*n* compounds are not conglomerates of enantiomorphous D and L crystals (which ought to melt eutectically, at lower temperatures), but rather true racemic crystals as shown in the following sections. Indeed, as explicitly claimed in the literature (p. 28 in ref. [20]), racemic compound crystals generally melt higher than their enantiomeric analogues; their greater thermodynamic stability originates from an increased structural compactness and symmetry. This is the case for the DL- and L-pyroglutamic acids, which have crystal densities of 1.492 and 1.440 g cm^{-3} and melting points of 184 °C and 162 °C, respectively, since their crystal structures are completely different.[19, 22] It is also essential to note that the melting of the crystals into smectic phases takes place at temperatures which increase with *n* only very slightly for DL*n*, whereas they increase considerably for L*n*. As discussed below, this behaviour suggests that the crystal stability of the racemic DL*n* is mainly controlled by the packing of the pyroglutamic moieties; the crystal stability of the optically active L*n* is dominated instead by the packing of the alkyl chains.

The melting enthalpies of the L*n* (taken from ref. [12]; note: the correct value of the *y* intercept is –12.8 instead of –2.8 as unfortunately printed in the literature) and DL*n* salts depend strongly on the length of the alkyl chains and increase linearly with *n* according to Equations (1) and 2 (Figure 2), which were established by a linear least-squares fit of the experimental data (with reliability factors *R* of 0.9997 and 0.9994, respectively).

$$\text{L}n\text{: } \Delta H\ [\text{kJ mol}^{-1}] = -12.8_{\pm 1.2} + 4.50_{\pm 0.08}n \qquad (1)$$

$$\text{DL}n\text{: } \Delta H\ [\text{kJ mol}^{-1}] = +7.8_{\pm 1.0} + 2.73_{\pm 0.07}n \qquad (2)$$

The *y* intercept of the ΔH versus *n* straight lines is clearly related to the melting of the pyroglutamate cores taken separately. The higher values measured for DL*n* (+7.8 kJ mol^{-1} for DL*n* and –12.8 kJ mol^{-1} for L*n*) indicate, just as was concluded above from the melting temperatures, that the packing of the pyroglutamate cores in the crystal is much more stable in the racemic than in the optically active series of compounds. Indeed, as emerges from simple thermodynamic considerations, the larger the amount of heat absorbed in a melting process, the smaller the enthalpy and the greater the stability of the starting crystal with respect to the resulting liquid. However, the sign of the *y* intercept is more important. The sign is positive for DL*n*, and reveals the strong cohesion of the crystal packing of the polar cores in the racemic case. On the other hand, the negative sign for L*n* indicates that the crystal packing of the optically active pyroglutamate cores is energetically unfavourable, and the crystals release part of their heat content upon melting. The pyroglutamate groups in the L*n* crystals must obviously be constrained either by the anchoring conditions imposed upon them by the ordered alkyl chains and/or by their electrostatic interactions.

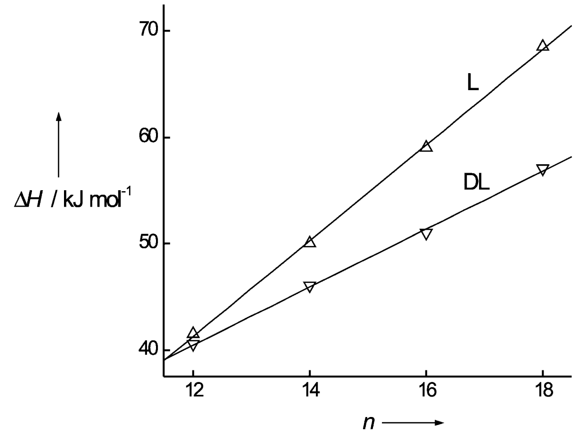

Figure 2. Chain length dependence of the enthalpies measured at the phase transition from the crystal into the smectic liquid crystal of the L*n* (△) and DL*n* (▽) compounds.

The slope of the ΔH versus *n* straight lines clearly represents the amount of heat necessary for the melting of the methylene groups. The slope measured for L*n* of about 4.5 kJ per methylene group compares well with that found for linear *n*-paraffins (4.1 kJ mol^{-1}),[19] denoting that the packing of the chains in the L*n* crystals is as strong as in conventional paraffin crystals. The measured slope for DL*n* (2.73 kJ mol^{-1}) is significantly smaller, denoting a constrained packing of the alkyl chains. Similar unconventional packing of alkyl chains which also led to a low melting enthalpy (2.6 kJ per methylene group) was recently reported in the literature for the Cu$^{\text{II}}$ soap crystals; here, instead of being packed as usual in a chevron-type arrangement, the alkyl chains were packed with the zigzag planes all parallel to one another (see Figure 4 in ref. [23]).

Molecular volume: The molecular volume was measured by dilatometry for several L*n* and DL*n* compounds in the smectic state. The volume in the crystalline state was disregarded because after degassing at high temperature (as required by the experimental technique), the solid samples recrystallized from the melt are out of equilibrium. The results obtained are summarized in the Equations (3)–(6) (reliability factor $R = 0.999$).

$$\text{L12: } V\ [\text{Å}^3] = 507.15_{\pm 0.05} + 0.3133_{\pm 0.0005}T[^\circ\text{C}] \qquad (3)$$

$$\text{L14: } V\ [\text{Å}^3] = 559.85_{\pm 0.09} + 0.3457_{\pm 0.0008}T[^\circ\text{C}] \qquad (4)$$

$$\text{DL14: } V\ [\text{Å}^3] = 555.97_{\pm 0.08} + 0.4097_{\pm 0.0007}T[^\circ\text{C}] \qquad (5)$$

$$\text{L18: } V\ [\text{Å}^3] = 652.33_{\pm 0.13} + 0.5420_{\pm 0.001}T[^\circ\text{C}] \qquad (6)$$

Firstly, within the experimental error (see Experimental Section), the molecular volume of L14 hardly differs from that of DL14 (at 125 °C, $V = 603_{\pm 6}$ Å^3 for L14 and $V = 607_{\pm 6}$ Å^3 for DL14), suggesting that chirality does not significantly affect the packing density in the smectic state. Secondly, the relative thermal expansion of the molecular volume, $(\partial V/\partial T)/V \cong + 7 \times 10^{-4}$ K^{-1}, is identical with that currently found for organic materials in the liquid state. Thirdly, the molecular volume increases linearly with the chain length, as expected from the well-known rule of additivity of the individual volumes of the component parts of the molecules according to Equation (7) (at 125 °C, reliability factor $R = 0.99998$).

$$V\,[\text{Å}^3] = 199.5_{\pm 2.5} + 28.93_{\pm 0.17} n \qquad (7)$$

Satisfactorily enough, the molecular volume of the methylene groups deduced from the slope of the corresponding straight line (28.9 Å^3) compares well with that currently found in the literature for liquid crystals (28.5 Å^3).[24]

Structure of the crystal phases: The thermotropic behaviour of the Ln and DLn compounds detected by polarizing optical microscopy and differential scanning calorimetry was confirmed by X-ray diffraction. The powder patterns recorded at low temperature contain a large number of Bragg reflections, all very sharp, indicative of a well-developed, three-dimensional crystal packing of the molecules. The (four) reflections located in the small-angle region follow each other with reciprocal spacings in the ratio 1:2:3:4, indicating that the molecules are arranged in superposed layers just as commonly observed with long-chain amphiphiles.[25]

A mere visual inspection of the diffraction patterns reveals immediately that the lamellar structure of the DLn is radically different from that of the optically active Ln compounds. This difference confirms the conclusion drawn from DSC that the DLn compounds are authentically racemic in nature. If they were not, the DLn compounds would produce X-ray patterns identical to those of the Ln compounds.

As is generally observed with long-chain amphiphiles in the solid state,[23–25] the lamellar structure of Ln and DLn compounds also consists of two sublayers periodically and alternately piled up in space: one containing the pyroglutamate cores and covered on both sides by the negative carboxylate ions, and one other containing the paraffin chains in a fully extended conformation and covered by the positive ammonium ions (Figure 3). The lamellar periods measured from the small-angle reflections represent the thickness of the two sublayers superposed. The temperature-independent periods d grow linearly with the number of carbon atoms n in the alkyl chains (Figure 4) according to Equations (8) and (9) (with reliability factors $R = 0.99999$ and 0.99987, respectively).[26]

$$\text{L}n\!: d\,[\text{Å}] = 9.09_{\pm 0.06} + 1.17_{\pm 0.01} n \qquad (8)$$

$$\text{DL}n\!: d\,[\text{Å}] = 6.92_{\pm 0.17} + 0.99_{\pm 0.01} n \qquad (9)$$

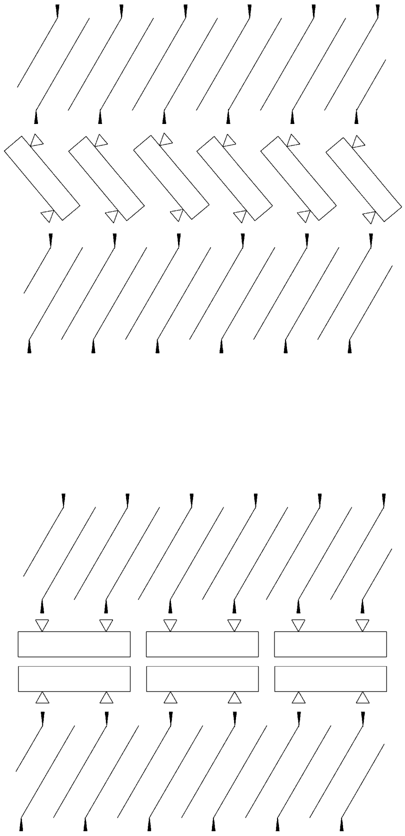

Figure 3. Schematic representation of the crystalline structure of the racemic DL (top) and the optically active L (bottom) n-alkylammonium salts of pyroglutamic acid.

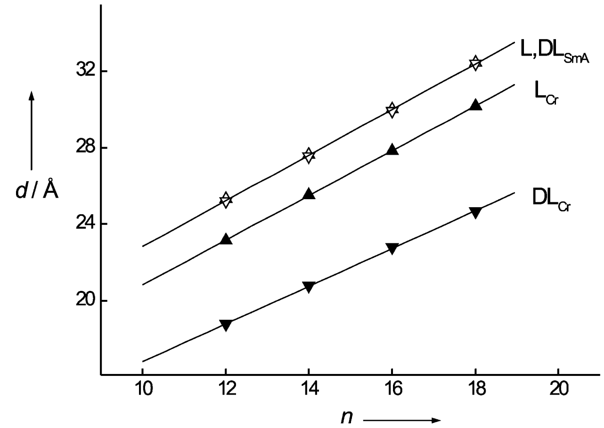

Figure 4. Chain length dependence of the lamellar period of the racemic DL (▼) and the optically active (▲) n-alkylammonium pyroglutamates in the crystalline and smectic A state (SmA).

The lamellar periods measured do not exceed half the overall length of the Ln and DLn dimers (as estimated by molecular modelling); this clearly indicates that the alkyl chains are interdigitated head to tail in single layers and tilted away from the layer normal as shown schematically in Figure 3. This arrangement is further substantiated by the slope Δd of the d versus n straight lines representing the rate of thickening of the crystalline lamellae per methylene group added to the molecules ($\Delta d = 1.17_{\pm 0.01}$ Å for Ln and $0.99_{\pm 0.01}$ Å for DLn), a slope which is effectively smaller than the length of one methylene group in an all-*trans* paraffin chain ($1.27_{\pm 0.01}$ Å per methylene group).[25] The slope Δd additionally permits one to calculate the tilt of the chains in the layers, $\theta = \cos^{-1}(\Delta d/1.27) = 22.7°$ for L*n* and 38.9° for DL*n*, and hence to get an estimate of the area covered in the layers by each alkyl chain, $S = \sigma/\cos\theta \cong 20.1_{\pm 0.5}$ Å^2 for L*n* and $23.8_{\pm 0.6}$ Å^2 for DL*n* (σ is the known cross-sectional area of paraffin chains in the crystalline state; $\sigma \cong 18.5_{\pm 0.1}$ Å^2).[25, 27] Quite interestingly, the area S is distinctly smaller in the optically active L*n* than in the racemic DL*n* compounds.

The y intercept of the d versus n straight lines, which corresponds to the thickness d_0 of the fictitious ammonium pyroglutamate layers, provides a direct measure of the thickness of the pyroglutamate sublayers in the lamellar L*n* and DL*n* crystals. The two thicknesses found ($9.09_{\pm 0.06}$ Å for L*n* and $6.92_{\pm 0.17}$ Å for DL*n*) are significantly different from each other and this indicates that the pyroglutamate cores are packed differently in the two series of compounds (Figure 3); this result is consistent with the difference found in the molecular area of the alkyl chains.

In the absence of complementary information that can only be obtained when properly grown single crystals are available (e.g. crystal lattice parameters, space group symmetry, electron density distribution), it is impossible to describe securely the detailed packing mode of the pyroglutamate groups in the polar sublayers and hence to specify the structural differences between the L*n* and DL*n* crystals. However, as a guide mark in the discussion, it is tempting to propose the following two schematic models, which stand out on simple stereochemical and geometrical grounds.

The first concerns the series of optically active L*n* compounds, in which the hydrogen-bonded molecules are by necessity all in the form of LL dimers. Since the carboxylate groups in the LL dimers both point to the same side with respect to the pyrrolidone plane (Figure 1), the LL dimers must logically lie parallel to the crystal layers and arrange themselves back to back as shown in Figure 3 (bottom); they can thus let the carboxylate groups point out of the polar sublayers and so come into contact, just as required by electrostatics, with the oppositely charged ammonium ions. This arrangement is all the more plausible as the thickness found for the pyroglutamate sublayers ($d_0 = 9.09$ Å) is close to that of two flat dimers superposed ($\approx 2 \times 4.4 = 8.8$ Å, Figure 1), and also as the area occupied in the layers by a pair of dimers, equal to that covered by four alkyl chains ($4 \times 20.1 = 80.4_{\pm 1.8}$ Å^2), is close to the lateral expanse of the dimers ($\approx 7 \times 11 = 77$ Å^2, Figure 1).

The second structural model concerns the series of racemic DL*n* compounds. In this case, the "racemic" structural repeat units may be either in the form of DL dimers or in the form of LL and DD dimers in equal numbers. In fact, the latter possibility cannot be retained here, for it would imply packings similar to those proposed for the L*n* compounds, which are inconsistent with the value of d_0 and S found experimentally. Since the carboxylate groups in the DL dimers point to opposite sides with respect to the average pyrrolidone planes (Figure 1), the DL dimers must in all likelihood be arranged in single layers as shown in Figure 3 (top); they must further be tilted away from the layer normal and also rotated to some degree about their long axis, so as to allow the carboxylate groups to sit properly on the surface of the polar sublayers in contact with the ammonium counterions. With a tilt of about 50°, this arrangement is perfectly consistent with the thickness of the pyroglutamate sublayers ($d_0 = 6.92$ Å) being close to the projected length of the dimers along the layers' normal ($\approx 11 \times \cos 50 = 7.07$ Å) and with the area covered in the layers by two alkyl chains ($2 \times 23.8 \approx 47.6_{\pm 1.2}$ Å^2) being close to that deduced from the cross-sectional area of the tilted dimers ($\approx 4.4 \times 7/\cos 50 = 47.9$ Å^2).

As suggested earlier, the greater thermodynamic stability of the racemic crystals with respect to their enantiomorphous analogues originates from their higher structural compactness. Since a direct measure of the molecular volume of the pyroglutamate groups in the crystals is out of the question in the present work (vide supra), the only way out is to calculate this volume indirectly. For that purpose, it suffices to take as a principle the well-known fact that in an homologous series of aliphatic compounds in the crystalline state the packing mode of the alkyl chains and terminal groups is reliably independent of the chain length.[25] This implies that the molecular area S (contribution of one molecule to the lateral spreading of the layers) and the molecular volumes V_{CH_2} and V_0 of the methylene and ammonium pyroglutamate groups are all independent of the number n of methylene groups in the chains. Therefore, the volume of one molecule, $V = V_0 + nV_{CH_2}$, and the thickness of one crystalline lamella, $d = V/S = (V_0/S) + n(V_{CH_2}/S)$, both grow linearly with n. Under this assumption, the molecular volume V_0 may easily be deduced from the ratio of the y intercept over the slope of the d versus n straight lines determined by X-ray diffraction. The values found ($V_0 = 7.8_{\pm 0.1} \times V_{CH_2}$ for L*n* and $7.0_{\pm 0.2} \times V_{CH_2}$ for DL*n*) are perfectly consistent with the conclusions drawn from the thermal behaviour of the DL*n* and L*n* series of compounds: the packing density of the racemic DL compounds is indeed higher than that of the optically active LL analogues (by $10_{\pm 4}$%). In addition, with the reasonable value of $V_{CH_2} = 1.27 \times 18.5 = 23.5$ Å^3,[25, 27] the density of the pyroglutamate groups in the polar sublayers is $1.33_{\pm 0.05}$ g cm^{-3} for L*n* and $1.47_{\pm 0.07}$ g cm^{-3} for DL*n*, which is in agreement with the values reported in the literature for the L- and DL-pyroglutamic acids (1.440 and 1.492 g cm^{-3}, respectively).[19, 22]

Structure of the smectic phases: The X-ray powder patterns of the racemic DL*n* compounds in the smectic state, like those of the optically active L*n* analogues,[12] contain three equidistant, sharp reflections in the small-angle region following each other with reciprocal spacings in the ratio 1:2:3, indicative of a smectic layering, and a broad band at 4.6 Å, related to the disordered conformation of the alkyl chains. The patterns are devoid of any other scattering signal, which indicates that both the alkyl chains and the pyroglutamate fragments inside the polar sublayers are arranged in a liquid-like fashion just as expected for a smectic A phase.

The smectic periods measured are virtually independent of temperature ($(\partial d/\partial T)/d = -4 \times 10^{-4}$ K^{-1}) and represent the thickness of one paraffin and one ammonium pyroglutamate sublayer superposed. With a steadily increasing number of carbon atoms in the alkyl chains, the periods of the DL*n* and L*n* compounds appear, for all practical purposes, to be equal to each other (Figure 4). Even when measured with the best accuracy possible under exactly the same experimental conditions,[26] they differ by less than 0.1 Å. Expressed analytically, they grow linearly as a function of n according to Equation (10) (125 °C, reliability factor $R = 0.99991$).

$$d\,[\text{Å}] = 10.87_{\pm 0.18} + 1.20_{\pm 0.01} n \qquad (10)$$

Combined with the molecular volumes measured by dilatometry, these periods permit one to calculate the molecular area $S = V/d$ (contribution of one molecule to the surface covered by the smectic layers) and the thickness $d_0 = V_0/S$ of the ammonium pyroglutamate sublayers (Figure 5). Contrary to what is observed in the crystal phases, in which they are strictly invariable for structural reasons, these parameters turn out to change very little but measurably with the length of the alkyl chains: S increases from 21.6 to 22.2 Å^2 and d_0 decreases from 9.2 to 9.0 Å when n goes from 12 to 18.

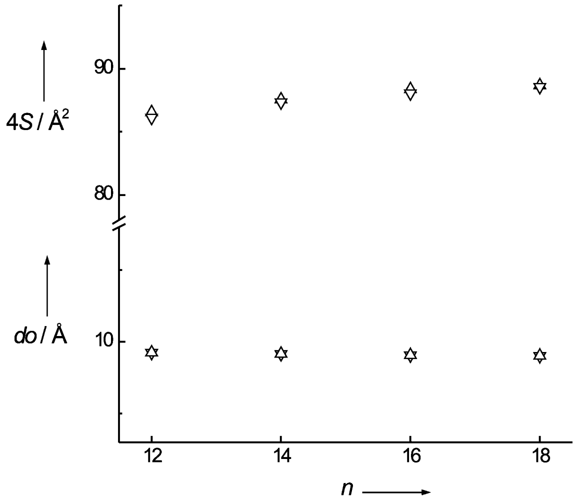

Figure 5. Chain length dependence of the thickness of the polar sublayers d_0 and the molecular area 4S of the racemic DL (▽) and the optically active L (△) *n*-alkylammonium pyroglutamates in the smectic A state.

In the case of the optically active L*n* compounds, the interpretation of the molecular arrangement in the smectic state is straightforward. As shown in Figure 4, the lamellar spacing increases very little at the transition from the crystal into the smectic phase. Specifically, it grows by only 9 %, an amount which reflects the 18 % volume expansion of the material [the molecular volume increases from $V_{cr} = S \times d = 20.1 \times (182.7 + 23.5n)$ to $V_{Sm} = 199.5 + 28.93n$] for a 9 % lateral expansion of the layers (the molecular area increases from 20.1 to about 22 Å^3). At the same time, the thickness d_0 of the polar sublayers (equal to 9.09 Å for the crystal and to 9.0–9.2 Å for the smectic phase) remains utterly unchanged. Despite the abrupt loss of the long-range positional ordering of the molecules inside the layers, the packing mode of the pyroglutamate dimers appears therefore to remain virtually unchanged, at least on a local scale. For the same geometrical reasons as prevailing for the crystal phases, related to the fact that the carboxylate groups in the LL dimers both point to the same side with regard to the pyrrolidone plane (Figure 1), the dimers must continue, therefore, to lie flat in the layers and arrange themselves back to back as shown in Figure 3 (bottom).

In the case of the racemic DL*n* compounds, the structure of the smectic phase seems, at first sight, more delicate to discuss. At the transition from the crystal to the smectic phases, the lamellar periods grow indeed by as much as 31–34 % (Figure 4), implying an important change of the local packing mode of the ammonium pyroglutamate moieties. Considering that the DL*n* compounds in the smectic state have precisely the same structural parameters (d, S and d_0), the same infrared spectra (vide supra), and practically the same clearing temperatures (Table 1) as their L*n* counterparts, it seems legitimate to conclude that they also have the same molecular packing. Turning from single to double layered (Figure 3), this packing implies that at the crystal-to-smectic phase transition the heterochiral DL dimers, such as found in the crystal, suddenly transform almost completely into a mixture of homochiral DD and LL dimers in equal numbers. Examples of such a polymorphic change of racemic crystals into pseudoracemic “solid” solutions upon heating have barely been reported in the literature as a result of the difficulties in interpretation of the experimental data (see p. 139 in ref. [20]).

This change of the supramolecular structure of the DL*n* dimers at the crystal-to-smectic phase transition may be acceptably understood on thermodynamic grounds by considering the prominent part taken in the minimization of free energy by enthalpy at low and entropy at high temperatures. Because the dimers in the smectic A layers are arranged in a liquid-like fashion and are thus released from the requirements of structural homogeneity of the racemic crystals, the D and L enantiomers are free to obey the laws of chemical equilibria ($2\mathrm{DL} \rightleftharpoons \mathrm{DD} + \mathrm{LL}$),[28] and hence to associate with one another through hydrogen bonding to develop pseudoracemic mixtures of DD, LL and DL dimers. In the low-temperature crystal, the attraction of the dimers is best satisfied, and therefore the enthalpy and free energy are most efficiently reduced to a minimum if the dimers are all heterochiral, because these are able, as it happens for symmetry reasons, to pack in a specially dense fashion (vide supra). In the high-temperature smectic phase, on the other hand, the entropy increases more, and therefore the free energy decreases to a lower minimum if at least part of the dimers are homochiral, because the entropy of melting is then increased with the entropy of mixing of the three types of dimer in the system. In the absence of discriminating interactions between the dimers (ideal mixture), chemical equilibrium should normally occur when the entropy of mixing is maximized, that is when the dimers, whose enthalpies of formation by hydrogen bonding are (most likely) identical, are in equal proportions. In reality, however, equilibrium is reached when the concentration of DL is reduced below ⅓ and conceivably even below ⅒, a value undetectable by the X-ray technique used in the present work. An obvious reason for such a behaviour is that for stereochemical reasons the heterochiral and homochiral dimers have difficulty in packing together (DD and LL lie flat in the layers, while DL stand at an angle, see Figure 3) and interact with one another unfavourably, thereby contributing a positive enthalpy of mixing and thus shifting the chemical equilibrium towards a further reduction of the less abundant heterochiral species. One other reason, less obvious at first sight but equally plausible as found below, is that the DD and LL homochiral dimers are liable to interact with one another favourably (like the two enantiomers in a racemic crystal), thereby contributing a negative enthalpy of mixing but also shifting the chemical equilibrium in the same direction as previously towards a reduction of the heterochiral species.

Binary mixtures of DL*n* with L*n*: The phase behaviour of the binary mixtures of the DL*n* and L*n* compounds was systematically investigated upon heating by differential scanning calorimetry, polarizing optical microscopy and X-ray diffraction. Figure 6 shows the phase diagram established for the binary mixture of the octadecyl derivatives taken as a typical example.

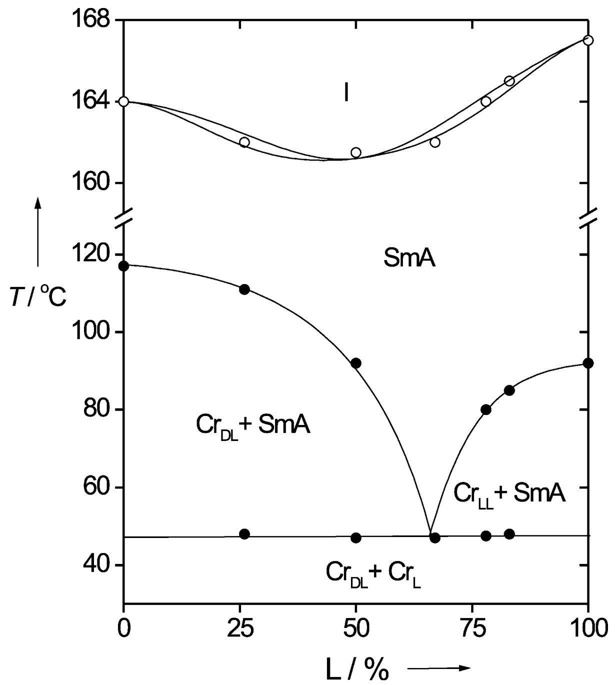

Figure 6. Binary phase diagram of the DL and L-octadecyl pyroglutamates.

It is important to note that no extra liquid crystal phases make their appearance in the binary mixtures, and that the smectic phases of the DL*n* and L*n* compounds are completely miscible at all compositions. This is plainly demonstrated by X-ray diffraction. With compounds comprising the same alkyl chains and hence the same smectic periods, these remain unchanged throughout the whole expanse of compositions; with compounds differing in chain length, they vary with composition in a continuous (practically linear) fashion between the periods of the pure DL*n* and L*n* compounds. This behaviour suggests that the smectic structure remains basically the same for all the binary mixtures; the D and L enantiomers continue to associate with one another to form predominantly homochiral DD and LL dimers.

The occurrence of the smectic phase upon heating proceeds through the eutectic melting of the DL*n* and L*n* crystals in the mixture. This melting is signalled by the presence in the DSC graphs of two distinct but connected endothermic peaks whose separation decreases monotonically with the distance to the eutectic composition. A sharp peak, located at the composition-independent eutectic temperature (47 °C), reveals the emergence of the smectic phase in the middle of the crystalline material, and an asymmetrical peak, located at the composition-dependent solidus temperature, signifies the completion of the melting process.[29] The very existence of a eutectic point, fully corroborated by optical microscopy and X-ray diffraction, is an indisputable indication that in the crystalline state the DL*n* compounds are neither conglomerates nor pseudoracemates, but true racemates involving repeat units made of the two enantiomers in equal numbers arranged according to a unique Bravais lattice. This is further substantiated by the fact that the solidus temperature, which corresponds to the complete melting of the racemic DL*n* crystals, goes through a maximum at the exact composition corresponding to pure DL*n*.

The full miscibility of the DL*n* and L*n* compounds in the smectic state is a clear indication that their smectic symmetry is identical (smectic A in both cases) and that the effective repulsion of their molecular components is not too strong.[30] For mixtures of compounds with the same chain length and therefore with the same clearing temperature (Table 1), the transition from the smectic into the isotropic liquid phase seems, when detected by DSC, to take place at a temperature which is independent of composition. However, in actual fact, when measured with great care by optical microscopy, the clearing temperature proves to proceed through a low maximum at a composition corresponding to pure DL*n* (Figure 6). This stabilization of the smectic phase with regard to the isotropic liquid suggests, as insinuated at the end of the previous section, that the enantiomeric homochiral DD and LL dimers, highly concentrated in mixtures rich in DL*n*, have a tendency to attract each other specifically, probably leading to the formation of a stoichiometric compound made of one DD and one LL dimer arranged back to back in the layers as shown in Figure 3 (bottom).

Conclusion

The long-chain alkylammonium pyroglutamates investigated in the present work are self-assembled in thermally stable, hydrogen-bonded dimers, which are crystalline at low temperature and smectic at high temperature. The lamellar structure of the racemic crystals is controlled by the packing of the ammonium pyroglutamate cores, while that of the optically active crystals is dominated instead by the packing of the alkyl chains. The dimers of the optically active compounds are homochiral and arranged in double layers both in the crystalline and the smectic state, wherein the ammonium pyroglutamate cores lie flat in the layers. In the racemic series of compounds, on the other hand, the dimers are either heterochiral or homochiral, depending upon whether they are arranged in a crystalline or a smectic fashion. The pairing of the two enantiomers is heterochiral in the crystalline state, producing achiral DL dimers standing tilted and densely packed in well-ordered single layers, whereas it is homochiral in the smectic state, producing achiral pairs of DD and LL dimers, arranged back to back and loosely packed side by side in double layers. This behaviour illustrates the importance of crystallization in supramolecular chemistry.[31] By drawing the molecules nearer together and so amplifying the role of interactions, crystallization has an effect on the chemical equilibrium of the reacting molecules, often resulting in a decisive control over the nature and architecture of the supermolecules formed. Quite interestingly, the smectic layering, even if less stringent than the crystalline ordering, is perfectly able to play a similar role; the reason is that, owing to the amphiphilic character of the compounds producing smectic phases, the constituent parts of the molecules, here the ammonium pyroglutamate cores and the alkyl chains, are indeed forced to pack in a special way, arranging themselves separately on both sides of well-defined interfaces.

Experimental Section

Materials: Optically active L- and racemic DL-pyroglutamic acids [(*S*)-(−)-2- and (±)-2-pyrrolidone-5-carboxylic acid] were obtained from Aldrich and recrystallized twice from ethanol. Their salts with normal dodecyl, tetradecyl, hexadecyl and octadecyl amines were prepared by dissolving equimolar quantities of the acid and the corresponding amine in ethanol and allowing them to react at room temperature. The precipitated salts were filtered and recrystallized from ethyl acetate. The formation of salts was confirmed with FTIR (protonated NH groups occur at 2800–2500 cm^{-1} and 2200 cm^{-1} for the primary amines, carboxylate groups at 1586 and 1390 cm^{-1}), ^{1}H NMR spectroscopy and elemental analysis [calcd (%) for $C_{17}H_{34}O_3N_2$ (314.47): C 64.93, H 10.90, N 8.91; found (L salt): C 65.04, H 10.96, N 8.87; found (DL salt): C 64.66, H 10.94, N 8.82; calcd (%) for $C_{19}H_{38}O_3N_2$ (342.52): C 66.63, H 11.18, N 8.18; found (L salt): C 65.94, H 11.45, N 8.05; found (DL salt): C 66.48, H 11.25, N 8.05; calcd (%) for $C_{21}H_{42}O_3N_2$ (370.58): C 68.06, H 11.42, N 7.56; found (L salt): C 67.96, H 11.58, N 7.52; found (DL salt): C 67.94, H 11.47, N 7.42; calcd (%) for $C_{23}H_{46}O_3N_2$ (398.63): C 69.30, H 11.63, N 7.03; found (L salt): C 69.30, H 11.80, N 6.92; found (DL salt): C 69.04, H 11.69, N 6.94].

Characterization techniques: Thermogravimetric experiments were performed with a TA TGA-2050 instrument operating under nitrogen with a heating rate of 10 °C min^{-1}. Optical rotation measurements were carried out by using a Perkin–Elmer 241 polarimeter. Liquid crystal textures were studied using a Leitz–Wetzlar polarizing microscope equipped with a hot-stage and a Linkam TMS 91 controller. Molecular volumes were measured using a homemade computer-driven dilatometer containing 1 g of carefully degassed sample. To avoid thermal degradation, special care was taken to maintain the samples at the lowest possible temperatures (below 140 °C), especially during the degassing process. The experimental error is estimated at about 10^{-4} ($\approx 0.5^3$) for molecular volumes measured on a relative scale (for the volume of a given sample at different temperatures) and at about 10^{-3} (≈ 5 Å^3) for volumes measured on an absolute scale (for different samples at a same temperature). Thermotropic polymorphism was investigated by using a TA DSC-10 differential scanning calorimeter with heating and cooling rates of 10 °C min^{-1}. FTIR studies were performed using a Nicolet Magna 550 spectrometer equipped with a VLT-2 variable-temperature sample holder (Research and Industrial Instruments Company). Crystal and liquid crystal structures were established by X-ray diffraction (Guinier focusing camera, CuKα_1 radiation from an INEL X-ray generator, powder samples in Lindemann capillaries, INSTEC hot-stage, INEL CPS-120 curved position-sensitive detector, diffraction patterns recorded with a 10-min exposure time). Binary mixtures of DL*n* and L*n* compounds were prepared by thorough mechanical mixing of the DL*n* and L*n* powders at room temperature. To reduce thermal degradation to a minimum, the clearing temperatures were measured by optical microscopy (a quick-acting technique) according to a well-defined experimental procedure (preliminary heating of the microscope hot-stage at 160 °C, sample introduction and heating at 10 °C min^{-1}, registering of clearing temperature at half melting).

Acknowledgement

This research was partially supported by the NATO collaborative research grant CRG972021 and by COST D11, Supramolecular Chemistry. The authors also thank Dr. Benoît Heinrich and Mr. Fabrice Mathevet for dilatometry experiments.

---

[1] M. Vacatello, V. Busico, *Mol. Cryst. Liq. Cryst.* **1981**, *64*, 127–132.

[2] G. H. Needham, R. D. Willett, H. F. Franzen, *J. Phys. Chem.* **1984**, *88*, 674–680.

[3] V. Busico, P. Corradini, M. Vacatello, *J. Phys. Chem.* **1982**, *86*, 1033–1034.

[4] V. Busico, P. Cernicchlaro, P. Corradini, M. Vacatello, *J. Phys. Chem.* **1983**, *87*, 1631–1635.

[5] J. D. Gault, H. A. Gallardo, H. J. Müller, *Mol. Cryst. Liq. Cryst.* **1985**, *130*, 163–177.

[6] C. M. Paleos, D. Tsiourvas, P. Dais, *Liq. Cryst.* **1989**, *5*, 1747–1755.

[7] D. Tsiourvas, C. M. Paleos, A. Skoulios, *Macromolecules* **1997**, *30*, 7191–7195.

[8] D. Tsiourvas, C. M. Paleos, A. Skoulios, *Macromolecules* **1999**, *32*, 8059–8065.

[9] C. M. Paleos, D. Tsiourvas, Angew. Chem. **1995**, *107*, 1839–1855; *Angew. Chem. Int. Ed. Engl.* **1995**, *34*, 1696–1711.

[10] T. Kato in *Handbook of Liquid Crystals* (Eds.: D. Demus, J. Goodby, G. W. Gray, H. W. Spiess, V. Vill), VCH, Weiheim, **1998**, Vol. 2B, Chapter XVII.

[11] C. M. Paleos, D. Tsiourvas, *Liq. Crystals* **2001**, *28*, 1127–1161.

[12] D. Tsiourvas, C. M. Paleos, A. Skoulios, *Liq. Cryst.* **1999**, *26*, 953–957.

[13] J. W. Goodby in *Handbook of Liquid Crystals* (Eds.: D. Demus, J. Goodby, G. W. Gray, H. W. Spiess, V. Vill), Wiley-VCH, Weiheim, **1998**, Chapter V, pp. 115–132.

[14] J. W. Goodby in *Ferroelectric Liquid Crystals: Principles, Properties and Applications* (Eds.: J. W. Goodby, R. Blinc, N. A. Clark, S. T. Lagerwall, M. A. Osipov, S. A. Pikin, T. Sakurai, K. Yoshino, B. Zeks), Gordon and Breach, Philadelphia, **1991**, pp. 158–247.

[15] J.-F. Li, J. J. Stott, E. A. Shack, X.-Y. Wang, R. G. Petschek, C. Rosenblatt, *Liq. Cryst.* **1997**, *23*, 255–261.

[16] K. Ema, M. Kanai, H. Yao, Y. Takanishi, H. Takezoe, *Phys. Rev. E* **2000**, *61*, 1585–1592.

[17] M. Z. Cherkaoui, J.-F. Nicoud, Y. Galerne, D. Guillon, *Liq. Cryst.* **1999**, *26*, 1315–1324.

[18] K. Mikami, T. Yajima, M. Terada, Y. Suzuki, I. Kobayashi, *Chem. Commun.* **1997**, 57–58.

[19] R. C. Weast (Ed.), *Handbook of Chemistry and Physics*, 56th ed., CRC Press, C-717–719, **1975**.

[20] J. Jacques, A. Collet, S. H. Wilen, *Enantiomers, Racemates, and Resolutions*, Krieger, Malabar, Florida, **1991**.

[21] L. J. Bellamy, *The Infrared Spectra of Complex Molecules*, Chapman and Hall, London, **1975**, 236.

[22] a) V. Pattabhi, K. Venkatesan, *J. Chem. Soc. Perkin Trans.* **1974**, *2*, 1085–1089; b) E. Van Zoeren, H. A. J. Oonk, J. Kroon, *Acta Cryst.* **1978**, *B34*, 1989–1900.

[23] M. Ibn-Elhaj, D. Guillon, A. Skoulios, A.-M. Giroud-Godquin, P. Maldivi, *Liq. Cryst.* **1992**, *11*, 731–744.

[24] D. Guillon, A. Skoulios, J. J. Benattar, *J. Phys., Paris* **1986**, 47, 133–138.

[25] A. I. Kitaigorodskii, *Organic Chemical Crystallography*, Consultants Bureau, New York, **1961**.

[26] In order to compare the crystal structure of the L*n* and DL*n* compounds, the X-ray patterns of L*n*, which have been analysed previously (see ref. [12]), were recorded all over again with the best accuracy possible, under exactly the same experimental conditions as used for DL*n*.

[27] J. M. Robertson, *Organic Crystals and Molecules*, Cornell University Press, Ithaca, **1953**.

[28] W. J. Moore, *Physical Chemistry*, Prentice-Hall, New Jersey, USA, **1972**, p. 279.

[29] Z. Sideratou, D. Tsiourvas, C. M. Paleos, A. Skoulios, *Liq. Cryst.* **1997**, *22*, 51 – 60.

[30] S. Chandrasekhar, *Liquid Crystals*, Cambridge University Press, Cambridge, Great Britain, **1992**.

[31] J.-M. Lehn, *Supramolecular Chemistry*, VCH, Weinheim, Germany, **1995**.

Received: March 25, 2003 [F4985]